Fluorinated and Iodinated Dopamine Agents: D2 Imaging Agents for PET and SPECT

S. Chumpradit, M. P. Kung,† J. Billings, R. Mach,‡ and H. F. Kung*

Departments of Radiology, Psychiatry, and Neurology, University of Pennsylvania, Philadelphia, Pennsylvania 19104

Received August 10, 1992

A novel series of dual-labeling D2 dopamine agents (labeled with either ^{18}F or ^{123}I for PET or SPECT imaging, respectively) was investigated. Two desired *f*luorinated and *i*odinated *d*opamine *a*gents, FIDA1, (*S*)-(−)-2-(2-fluoroethoxy)-5-iodo-3-methoxy-*N*-[(1-ethyl-2-pyrrolidinyl)methyl]-benzamide, and FIDA2, (*R*)-(+)-2,3-dimethoxy-5-iodo-*N*-[(1-(4′-fluorobenzyl)-2-pyrrolidinyl)-methyl]benzamide, were synthesized. Both compounds displayed high affinity to the D2 receptor of rat striatal membrane preparations (K_d = 0.13 and 0.02 nM for FIDA1 and FIDA2, respectively). The biodistribution study in rats exhibited high localization in the striata of the brain with the striatum/cerebellum ratio reaching 29.3 and 13.1 at 1 h post iv injection for FIDA1 and FIDA2, respectively. Imaging studies with [^{18}F]- and [^{123}I]FIDA2 in monkeys, with PET and SPECT, respectively, showed comparable high selective striatal uptake. These results suggest that they are potentially useful D2 dopamine receptor imaging agents for PET and SPECT.

In vivo imaging of the dopaminergic system in the mammalian brain has been the subject of extensive studies in recent years. The dopaminergic system is important for normal brain function and is also a possible primary action site for various antiparkinsonian agents or neuroleptic drugs. There is an abundance of pharmacological information about the dopamine receptor.[1,2] A large number of CNS receptor imaging agents for single photon emission computed tomography (SPECT) and positron emission tomography (PET) imaging have been reported.[3-8] In vivo imaging techniques provide a powerful tool for the evaluation of CNS function in normal or disease states.

Imaging studies of CNS D2 dopamine receptors in humans using [^{11}C]raclopride with PET have been reported.[9,10] A high ratio of specific striatal to nonspecific cerebellar binding in living human brain was observed. Using an equilibrium model and Scatchard plots, the affinity constant (K_d = 7.1 nM, B_{max} = 15 pmol/mL) in living human brain was measured. The values for dopamine D2 receptor density were comparable to those determined earlier with a different imaging agent, *N*-methylspiperone (K_d = 0.097 nM, B_{max} = 16.6 pmol/g).[11] However, a different receptor concentration was reported based on quantitative in vivo imaging studies of schizophrenic patients with [^{11}C]-*N*-methylspiperone (NMSP)[7,11-13] and [^{11}C]raclopride.[9,10] NMSP showed a higher D2 dopamine concentration and raclopride displayed no change in dopamine receptor density. The results from the two different research groups on two different patient populations are controversial. This discrepancy may be a result of variations in the differential effects of endogenous dopamine concentration between raclopride and NMSP.[14,15] In addition, differences due to methodology and/or patient population have been suggested.[16] When the same patients were studied with either raclopride or NMSP, D2 receptor density appeared to be the same.[17]

Despite the attractive features associated with PET studies, this technique is still limited to a handful of major university medical centers and national laboratories, where an abundance of technical and financial resources is available. For the majority of nuclear medicine clinics, SPECT and planar imaging studies are the only procedures currently available. Generally, it is well-recognized that PET has higher resolution, higher sensitivity, and better quantitation capability than SPECT.[18] The resolution of SPECT (full width at half-maximum, fwhm, 7–15 mm) is generally lower than that of PET (fwhm, 4–7 mm). However, SPECT is more readily available, less expensive to perform, and less demanding technically, because it does not require an on-site cyclotron. Therefore it is more suitable for routine clinical studies.

A variety of substituted benzamide derivatives possessing antidopaminergic properties have been reported (Table I).[19-22] Of these many agents, raclopride,[10,23,24] IBZM,[25] IBF,[26,27] epidepride,[28,29] 5-fluoropropylepidepride,[30-33] and ioxipride (NCQ298)[34,35] show specific D-2 antagonistic activity and high affinity (lower K_d) in rat striatum tissue preparations as well as low nonspecific binding. Three types of iodinated compounds have been reported as D2 dopamine SPECT imaging agents: iodobenzamides (see Table I), iodospiperone,[36,37] and iodolisuride.[38,39] However, due to their higher selectivity and better affinity, more clinical studies of D2 dopamine receptors with SPECT have been performed using the iodinated benzamide derivatives.

Initial imaging studies in humans with [^{123}I]IBZM,[40-45] IBF,[26,46] and epidepride[28] demonstrate that these agents, as expected, localize in the basal ganglia area. SPECT imaging of normal human brain displayed a pattern that clearly delineated the location of the basal ganglia in the brain. In patients with Parkinsonian and other related movement disorders, [^{123}I]IBZM–SPECT imaging studies appear to provide important differential diagnosis for patient management.[41,44,47]

In order to maximize the effort and minimize the cost of drug development, we investigated a unique series of dual-labeling D1 and D2 postsynaptic imaging agents, which can take advantage of the best of both modalities—PET and SPECT. Data derived from PET and

* Address correspondence to: Hank F. Kung, Ph.D., Department of Radiology, University of Pennsylvania, Rm 305, 3700 Market Street, Philadelphia, PA 19104. (215) 662-3096.
† Department of Psychiatry.
‡ Department of Neurology.

0022-2623/93/1836-0221$04.00/0

Table I. Chemical Structures of Benzamides

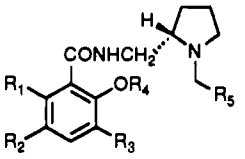

compd	R_1	R_2	R_3	R_4	R_5	K_d or K_i (nM)	ref
iodosulpiride	I	SO_2NH_2	H	CH_3	CH_3	1.5	3, 38
raclopride	OH	Cl	Cl	CH_3	CH_3	1.1	24
eticlopride	OH	Et	Cl	CH_3	CH_3	0.09	24, 19
IBZM	OH	I	H	CH_3	CH_3	0.43	60, 61
iodopride	H	I	H	CH_3	CH_3	3.0	19
epidepride	H	I	OCH_3	CH_3	CH_3	0.025	28, 29
ioxipride (NCQ298)	OH	I	OCH_3	CH_3	CH_3	0.019	35, 38
IBF	H	I		$-CH_2CH_2-$	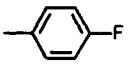	0.106	26, 27
NCQ115	H	Br	OCH_3	CH_3		0.147	51
NCQ616	H	Br	OCH_3	CH_2CH_2F	CH_3		51
FP-epidepride	H	$(CH_2)_3F$	OCH_3	CH_3	CH_3	0.02	30, 31
FEOB	H	H	OCH_3	CH_2CH_2F	CH_3	13	50

SPECT studies cannot be readily compared because different ligands are required. The incompatibility is due to the fact that different agents are used for each modality. Although in many cases these ligands are close analogs, they are not the same molecule, and therefore pharmacokinetic and metabolic differences prevent their cross-comparison. Earlier reports by Wilson et al.[48,49] demonstrated the feasibility of using [^{11}C]- and [^{125}I]IMB as a dual-labeled agent for CNS D2 receptor imaging. However, the agent is not ideal and the physical half-life of the ^{11}C-labeled agent ($T_{1/2}$ = 20 min) may be too short for a full-scale pharmacokinetic analysis.

To bridge the gap between SPECT and PET imaging techniques and to enhance the potential of a single radiopharmaceutical for clinical application, two dual-labeling benzamides, *f*luorinated and *i*odinated *d*opamine *a*gents (FIDA), as D2 dopamine imaging agents, which can be labeled with either ^{18}F and ^{123}I on the same molecule for both PET and SPECT, were prepared and evaluated. The design of these molecules was based on several considerations: they should be highly selective and have good affinity for D2 receptors, they should be readily labeled with ^{18}F and ^{123}I on the same molecule, and the corresponding ^{18}F and ^{123}I-labeled compounds should have a similar in vivo metabolism. There are a number of interesting lead compounds which suggest that it is possible to modify the benzamides to have such desired properties. Replacement of the 2-methoxyl group with a 2-fluoroethoxy group, gives an analog (FEOB)[50] with a K_i of 13 nM; similarly, the *N*-benzyl derivative, NCQ 115, shows a K_i of 0.143 nM (Table I). The function of this study is to determine whether the corresponding 5-iodo analogs of FEOB (to give FIDA1, 4) and NCQ115 (to give FIDA2, 6)

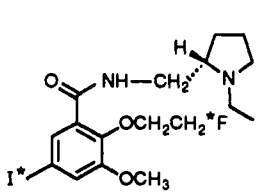

S-(−)-FIDA1

4

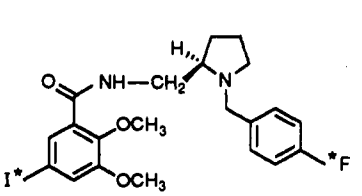

R-(+)-FIDA2

6

have the desired properties for D_2 receptor studies in vivo with PET and/or SPECT. It is important to note that for the *N*-benzyl derivatives, the *R*-(+) is the preferred conformation for D2 dopamine receptor affinity, while the (*S*)-(−)-*N*-ethyl-substituted benzamides displayed the desired higher affinity.[20,51]

Scheme I. Synthesis of FIDA1 and FIDA2

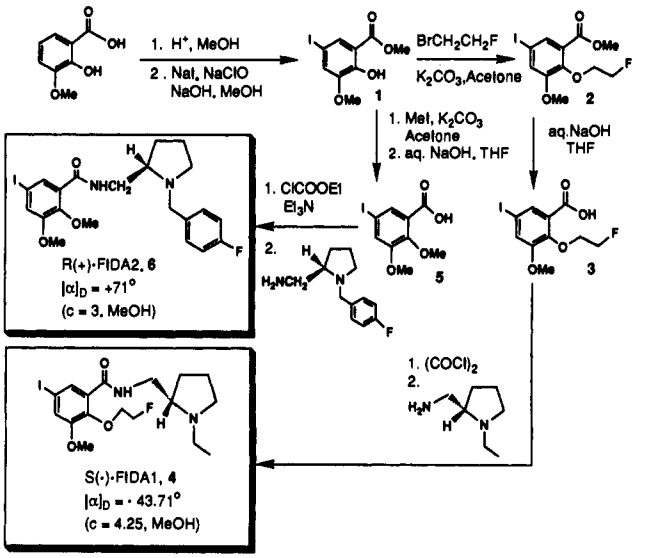

Chemistry

Preparation of FIDA1 and FIDA2 was achieved as shown in Scheme I. The iodinated ester 1 was prepared by iodination of the corresponding methyl ester of 3-methylsalicylic acid using sodium iodide in the presence of sodium hypochlorite as an oxidant.[52] O-Alkylation of 1 with 1-bromo-2-fluoroethane or methyl iodide, followed by basic hydrolysis, afforded the acid 3 or 5, respectively. Treatment of acid 3 with oxalyl chloride produced the acid chloride,[30] which was reacted with (*S*)-(−)-*N*-ethyl-2-(aminomethyl)pyrrolidine (200% mol) in dichloromethane to give amide 4 (FIDA1). In order to conserve the pyrrolidine base, which is an optically active starting material in limited supply, 6 (FIDA2) was synthesized by performing a one-pot reaction using triethylamine as the base. The activated ester of 5 was prepared by reacting it with ethyl chloroformate in the presence of triethylamine, followed by the addition of the mixture of (*R*)-(+)-*N*-(4-fluorobenzyl)-2-(aminomethyl)pyrrolidine[53] (1.0 equiv) and triethylamine (Scheme I). Both benzamide formation methods gave >80% yield of the respective final

Scheme II. Preparation of [^{123}I] or [^{125}I]-*S*-FIDA1 and -*R*-FIDA2

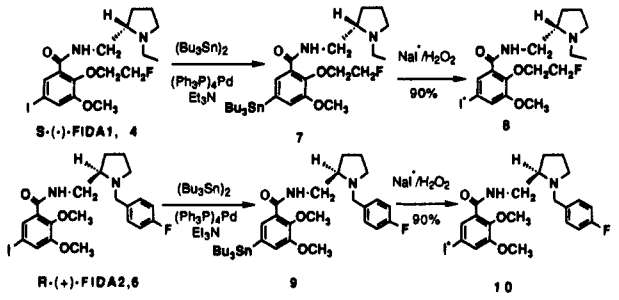

Scheme III. Synthesis of the Precursor of [^{18}F]-*R*-FIDA2

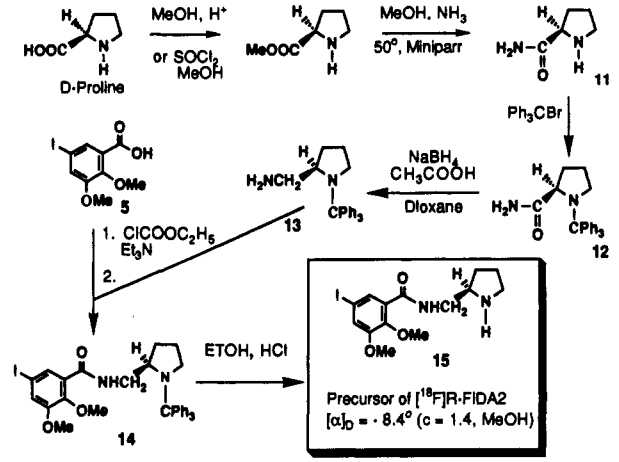

products. The optical purities of FIDA1 and FIDA2 were determined by high-pressure liquid chromatography (HPLC) fitted with a chiralcel OD column. Using a chiral column (chiracell-OD) and 10% ethanol/*n*-hexane, at a flow rate of 1 mL/min, *R*-(+)- and *S*-(−)-FIDA1 displayed retention times of 10.5 and 12.2 min, respectively. Under the same conditions, *R*-(+)- and *S*-(−)-FIDA2 showed retention times of 11.9 and 16.4 min, respectively. The sensitivity of the HPLC–chiral column method for measurement of optical purity is <1%.[54]

The precursors for radioiodination, tributyltin derivatives **7** and **9**, were synthesized by heating a mixture of FIDA1 or FIDA2, bis(tributyltin), tetrakis(triphenylphosphine)palladium, and palladium(II) acetate in triethylamine at 80–90 °C overnight (Scheme II). The reaction produced the same result in either the presence or absence of palladium(II) acetate.

The precursor, **15**, prepared as in Scheme III, was employed for radiolabeling with [^{18}F]-4-fluorobenzyl iodide to produce [^{18}F]FIDA2. D-(+)-*N*-Tritylprolinamide, **12**, was synthesized by N-benzylation with triphenylmethyl bromide in the presence of triethylamine.[55] The reduction of **12** to **13** was achieved by using sodium borohydride and acetic acid with dioxane as the solvent. The reaction gave a low percentage yield, most likely due to steric hindrance produced by the neighboring *N*-trityl group. The amine **13** was easily separated from the starting amide by column chromatography, and the amide **14** was synthesized in the same manner as that described for the preparation of **6** (Scheme I). The trityl group of **14** was removed by the addition of hydrogen chloride in ethanol; the desired amide, **15**, was obtained in good yield.

The amide **14** showed an optical rotation value of $[\alpha]_D$ = −8.40° (*c* = 1.4, MeOH). Subsequently, in a repeated

Scheme IV. Preparation of [^{18}F]-*R*-FIDA2

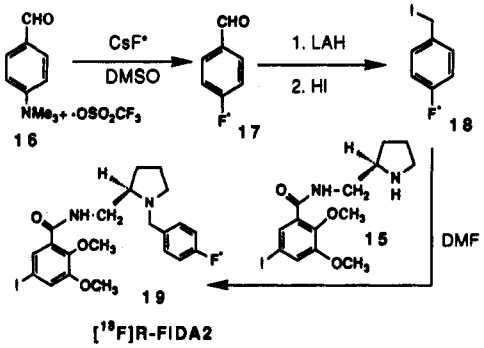

run of this reaction scheme, the amide **14** was obtained with a strikingly different optical rotation value of $[\alpha]_D$ = −3.30° (*c* = 1.96, MeOH). The chromatograms (HPLC, chiralcel OD) showed that **14** from the first run had 100% optical purity, but the second batch of **14** showed only 78% optical purity, indicating that racemization had occurred, most likely during the reduction step, from **12** to **13**. However, in a related reaction we found that the sodium borohydride–acetic acid mixture effectively reduced *R*-(+)-1-(4-fluorobenzyl)propylamide to *R*-(+)-2-(aminomethyl)-1-(4-fluorobenzyl)pyrrolidine without racemization. A similar finding using this same reagent was also reported in the literature.[53] Racemization of the reduction of (*S*)-1-(4-trityl)prolinamide to (*S*)-(−)-2-(aminomethyl)pyrrolidine using lithium aluminium hydride was also reported previously.[55] Comparing the two related reduction reactions mentioned above in which optical racemization was observed, it is apparent that the bulkiness of the *N*-trityl group may be the cause of racemization.

Radiolabeling. (1) Radioiodination. The radioiodination of compound **7** or **9** with ^{125}I at a no-carrier-added level was accomplished by an electrophilic iodination reaction using hydrogen peroxide as an oxidant.[56,57] The radiolabeled compound [^{125}I]-**8**, or -**10** was readily separated from the starting material, the tin compound, by HPLC purification. The retention time for [^{125}I]-**8** or -**10** was 4.6 and 9.0 min, respectively, as compared with that of the starting tin compound **7** or **9**, 15 and 30 min, respectively (PRP-1 column; solvent, acetonitrile/5 mM 3,3′-dimethylglutarate buffer, pH 7.0 at 90/10, v/v; flow rate, 1 mL/min). The overall yield of the no-carrier-added **8** or **10** was 85–90% (radiochemical purity >97%; no detectable UV material). [^{125}I]-**8** or -**10** was compared with the chemically pure, nonradioactive authentic compound by HPLC using simultaneous UV and radioactive detections. They were determined to be the desired product on the basis of their identical elution profile. The specific activity of the final product was assumed to be 2200 Ci/mmol. The same procedure was successfully applied to the radioiodination with ^{123}I, and the radiolabeling yields were comparable to those observed for the ^{125}I compounds.

(2) ^{18}F Labeling. Compound **15** was N-benzylated with [^{18}F]fluorobenzyl iodide **18** in DMF.[58,59] The product was purified by HPLC to give the desired compound **19** with 10% overall yield (EOS) (Scheme IV), specific activity ~800 μCi/mmol, and radiochemical purity >99% (no detectable UV material) as determined by HPLC.

In Vivo Biodistribution in Rats. After an iv injection of [^{125}I]FIDA1 in rats, moderate brain uptake (0.41% dose/organ at 2 min) was observed (Table II). At later time points, a large portion of the radioactivity was washed out

Table II. Biodistribution of [^{125}I]FIDA1, 4, in Rats after Intravenous Injection

organ	% dose/organ[a]			
	2 min	30 min	60 min	120 min
blood	3.76 ± 0.42	1.91 ± 0.58	0.78 ± 0.06	0.51 ± 0.04
heart	0.81 ± 0.18	0.14 ± 0.01	0.03 ± 0.01	0.01 ± 0.00
muscle	11.83 ± 4.03	8.24 ± 1.65	1.96 ± 0.18	0.76 ± 0.03
lung	6.53 ± 0.43	0.66 ± 0.06	0.14 ± 0.03	0.04 ± 0.00
kidney	6.18 ± 1.22	1.42 ± 0.32	0.39 ± 0.03	0.11 ± 0.01
spleen	0.70 ± 0.16	0.31 ± 0.05	0.05 ± 0.02	0.01 ± 0.00
liver	20.46 ± 5.46	22.40 ± 6.33	7.08 ± 1.93	2.24 ± 0.20
skin	8.19 ± 2.98	4.97 ± 1.12	1.76 ± 0.47	0.75 ± 0.13
thyroid	0.07 ± 0.00	0.03 ± 0.00	0.04 ± 0.02	0.03 ± 0.03
brain	0.41 ± 0.04	0.11 ± 0.01	0.05 ± 0.02	0.02 ± 0.00
	Regional Uptake[a]			
cerebellum	0.16 ± 0.02	0.03 ± 0.00	0.006 ± 0.00	0.0016 ± 0.00
striatum	0.30 ± 0.04	0.24 ± 0.05	0.175 ± 0.05	0.095 ± 0.03
hippo-campus	0.25 ± 0.05	0.05 ± 0.01	0.007 ± 0.00	0.0006 ± 0.00
cortex	0.25 ± 0.03	0.05 ± 0.01	0.013 ± 0.00	0.0014 ± 0.00
ST/CB	1.8	8.2	29.3	60.7

[a] Average of three rats. [b] Expressed as % dose/gram.

Table III. Biodistribution of [^{125}I]FIDA2, 6, in Rats after Intravenous Injection

organ	% dose/organ[a]			
	2 min	30 min	60 min	120 min
blood	2.08 ± 0.38	0.87 ± 0.14[b]	0.64 ± 0.08	0.46 ± 0.08
heart	1.38 ± 0.22[b]	0.16 ± 0.03[b]	0.06 ± 0.01	0.03 ± 0.00
muscle	11.14 ± 1.56	10.87 ± 0.77[b]	4.21 ± 0.64	2.04 ± 0.30[b]
lung	7.82 ± 0.34	1.06 ± 0.02[b]	0.32 ± 0.06	0.15 ± 0.01
kidney	6.77 ± 0.59	2.96 ± 1.55	1.38 ± 0.20	0.42 ± 0.06
spleen	1.19 ± 0.25	0.43 ± 0.01[b]	0.14 ± 0.01	0.05 ± 0.00
liver	19.41 ± 4.79	12.69 ± 0.98[b]	10.44 ± 2.40	5.71 ± 1.04
skin	6.08 ± 1.94	7.04 ± 1.44[b]	8.56 ± 1.84	5.75 ± 1.00
thyroid	0.07 ± 0.02	0.04 ± 0.01[b]	0.03 ± 0.01	0.03 ± 0.01
brain	0.98 ± 0.12	0.21 ± 0.04[b]	0.10 ± 0.03	0.05 ± 0.00
	Regional Uptake[c]			
cerebellum	0.49 ± 0.08	0.09 ± 0.01[b]	0.03 ± 0.01	0.01 ± 0.00
striatum	0.59 ± 0.08	0.40 ± 0.07[b]	0.37 ± 0.11	0.23 ± 0.03
hippo-campus	0.47 ± 0.10	0.14 ± 0.01[b]	0.05 ± 0.01	0.01 ± 0.00
cortex	0.63 ± 0.16	0.14 ± 0.02[b]	0.04 ± 0.01	0.01 ± 0.00
ST/CB	1.20	4.4	13.1	25.2

[a] Average of three rats. [b] Number of rats = 2. [c] Expressed in % dose/gram.

from brain (0.05% dose/organ at 1 h postinjection). The liver uptake remained high for the first 30 min and rapidly washed out 1 hr postinjection. The target to nontarget ratio in brain (striatum contains a high density of D2 dopamine receptors, while cerebellum is essentially devoid of D2 dopamine receptors) was determined by regional dissection. The striatum/cerebellum (ST/CB) ratio of [^{125}I]FIDA1 dramatically increased with time: 8.26, 29.3, and 60.7 at 30, 60, and 120 min, respectively (Table II). This type of profound increase in target to nontarget ratio vs time was not observed for the other two regions, hippocampus and cortex (Table II). These results suggest that in regions with nonspecific association, i.e. regions low in dopamine receptors, the agent is washed out rapidly, whereas the striatum (rich in dopamine receptors) shows prolonged retention.

[^{125}I]FIDA2 exhibited higher brain uptake (0.98% dose/organ at 2 min postinjection) in rats than [^{125}I]FIDA1 (Table III). Similarly, the radioactivity was also washed out from the brain (0.10% dose/organ at 1 h postinjection). High initial uptake in the liver was also observed, but the clearance of radioactivity was slower than that of [^{125}I]-FIDA1. The ST/CB ratio of [^{125}I]FIDA2 showed a gradual increase, from 1.2 at 2 min to 25.2 at 120 min. The studies on ex vivo autoradiography of these compounds (data not shown) also confirmed the selective regional distribution with high striatal localization reflecting D2 dopamine receptor distribution.

Table IV. Inhibition Constants of Compounds on [^{125}I]FIDA1 and [^{125}I]FIDA2 Binding to Rat Striatal Membranes[a]

compd	receptor type	K_i (nM)	
		FIDA1, 4	FIDA2, 6
spiperone	D2 antagonist	0.02 ± 0.003	0.03 ± 0.01
eticlopride	D2 antagonist	0.014 ± 0.002	0.06 ± 0.005
(+)-butaclamol	D2 and D1	1.05 ± 0.12	0.40 ± 0.02
raclopride	D2 antagonist	2.31 ± 0.43	5.0 ± 0.8
SCH23390	D1 antagonist	460 ± 38	536 ± 33
WB 4101	α1-adrenergic	33.1 ± 1.5	23.2 ± 2.2
yohimbine	α2-adrenergic		505 ± 70
quinpirole	DA agonist	2053 ± 410	8000 ± 1600
dopamine	DA agonist	1437 ± 175	5268 ± 1000
atropine	cholinergic	>10000	>10000
naloxone	opiate	>10000	>10000
5-HT	5-HT	>5000	>3000
(±)-propanolol	β-adrenergic	>10000	

[a] K_d values for FIDA1 and FIDA2 were 0.13 and 0.02 nM, respectively.

Since [^{125}I]FIDA2 showed a higher brain uptake than [^{125}I]FIDA1, FIDA2 was chosen for ^{18}F labeling and PET imaging in monkeys.

Binding Study. Competition study with various types of receptor ligands indicated that [^{125}I]FIDA1 and [^{125}I]-FIDA2 specifically bind to the dopamine D2 receptor with high selectivity (Table IV). The K_d values for FIDA1 and FIDA2 were 0.13 and 0.02, respectively. The rank order of inhibition for the binding of [^{125}I]FIDA1 and [^{125}I]-FIDA2 to the membrane preparations of rat striata by antagonists was consistent with the pharmacology of D2 receptors (Table IV); i.e., only D2 selective ligands showed high affinity for [^{125}I]FIDA1 and [^{125}I]FIDA2 binding, while the compounds selective for other receptors showed relatively low affinity. Thus, the selective antagonists spiperone, raclopride, and eticlopride were more potent than (+)-butaclamol, WB4101, yohimbine, ketanserin, and SCH-23390, but they were less potent as inhibitors. (−)-Butaclamol, naloxone, and propranolol showed little inhibition toward the binding of [^{125}I]FIDA1 and [^{125}I]-FIDA2. All of the ligands used in this study displaced [^{125}I]FIDA1 and [^{125}I]FIDA2 binding with pseudo-Hill coefficients close to 1.0, with the exception of dopamine as a D2 agonist, which may have two-site binding. The introduction of fluorine and iodine atoms in the same benzamide molecule appears to retain the D2 dopamine receptor binding affinity.

In Vivo Monkey Imaging

SPECT imaging of monkey brain using a triple-headed γ camera after iv injection of [^{123}I]FIDA2 can clearly delineate the basal ganglia as discrete structures 1 h after imaging. The target to nontarget (basal ganglia to remaining brain structures) ratio increases with time. Both [^{123}I]FIDA2 and [^{18}F]FIDA2 (done in the same monkey once on two different days) show high initial uptake in the monkey brain with moderate uptake in the soft tissues of the head and neck (images not shown). The combined regional distribution data from PET and SPECT strongly suggest that in the same monkey these two modalities with FIDA2, 6, which has both fluorine and iodine on the same molecule, show closely similar brain uptake and washout (Figure 1). Initial metabolite analysis of plasma from the monkey after the injection of [^{123}I]FIDA2 or [^{18}F]-

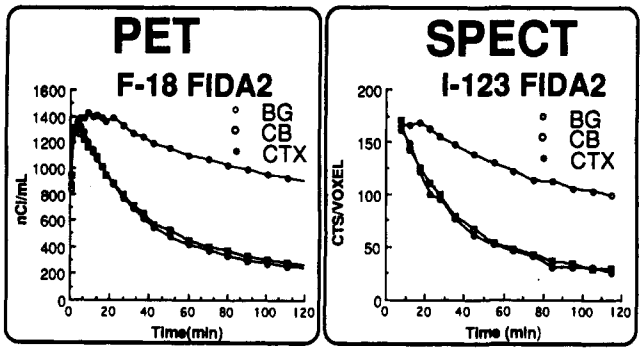

Figure 1. Comparison of [^{125}I]FIDA2 (by SPECT imaging) and [^{18}F]FIDA2 (PET imaging) uptake and washout curves from basal ganglia (BG), cortex (CTX), and cerebellum (CB) of monkey brain.

FIDA2 shows different metabolism rates. The [^{18}F]FIDA2 appears to show a faster metabolic rate than that observed for [^{123}I]FIDA2 (data not shown). However, the regional brain uptake and washout of FIDA2 appears to be the same with either [^{123}I]FIDA2 or [^{18}F]FIDA2. Additional studies are needed to validate the kinetics of metabolism and to evaluate the quantitative modeling of D2 receptor density in vivo.

In conclusion, preliminary data suggest that this series of compounds, which can be labeled with either ^{18}F for PET or ^{123}I for SPECT imaging, are potentially useful D2 dopamine receptor imaging agents for PET and SPECT. Ultimately, this approach may lead to the development of a simple and useful imaging procedure for studying the D2 receptor with either PET or SPECT. By using the same molecule for two imaging modalities, one can expect the same pharmacological profile, toxicology, and pharmacokinetics (to the extent that the biodistribution of the ^{123}I- and ^{18}F-labeled parent compound is the same). However, the similarities and differences of the biodistribution of metabolite(s) of different ^{123}I and ^{18}F moieties will have to be investigated and validated.

Experimental Section

General Methods. NMR were recorded on a Varian EM 360A, a Bruker WM-250 (250 MHz), or a Bruker AM 500 (500 MHz) spectrometer. The chemical shifts were reported in ppm downfield from an internal tetramethylsilane standard. Infrared spectra were obtained with a Mattson Polaris FT-IR spectrophotometer. Melting points were determined on a Meltemp apparatus and are reported uncorrected. HPLC was performed on Model Rabbit HP from Rainin Instrument Co., Inc. (Emeryville, CA) using a chiral column (chiralcel-OD, 4.1 × 250 mm; Diacel Inc., Los Angeles, CA). The optical rotation of compounds was measured on a Perkin-Elmer 243B polarimeter. Mass spectra were recorded on the mass spectrometer VG 70-70 HS with chemical ionization (CI), using methane or ammonia gas. Elemental analyses were performed by Atlantic Microlabs, Inc., of Norcross, GA, and were within 0.4% of the theoretical values.

Materials. Dichloromethane was refluxed and distilled from calcium hydride. D-Proline, L-proline, 3-methoxysalicyclic acid, oxalyl chloride, and ethyl chloroformate were purchased from Aldrich (Milwaukee, WI) and were used without further purification. (*S*)-(−)-*N*-ethyl-2-(aminomethyl)pyrrolidine was obtained from the resolution of (*RS*)-(±)-*N*-ethyl-2-(aminomethyl)-pyrrolidine according to the published procedure.[60,61] (*R*)-(+)- and (*S*)-(−)-2-(aminomethyl)-1-(4-fluorobenzyl)pyrrolidine were synthesized according to the literature.[53]

Methyl 5-Iodo-3-methoxysalicylate (1).[52] The esterification of 3-methoxysalicylic acid was performed according to the literature.[30,62] The ester product (1.68 g, 9.20 mmol) was dissolved in methanol (35 mL). Sodium iodide (1.38 g, 9.20 mmol) and sodium hydroxide (0.34 g, 9.2 mmol) were added, and the solution was cooled to 0 °C. To this solution was added aqueous sodium hypochlorite (17.25 g, 5% NaClO) dropwise. The colorless slurry mixture was stirred for 1 h at 0–3 °C and then treated with 10% aqueous sodium thiosulfite. The mixture was adjusted to pH 7 using 5% aqueous HCl. Ether (50 mL) was added, and the layers were separated. The ether layer was washed with brine and dried over anhydrous sodium sulfate. After the ether was evaporated, the crude orange solid was purified by column chromatography (silica gel, $CHCl_3$) to obtain 1.2 g (43%) of the iodo product: mp 104 °C (lit.[62] mp, 110–112 °C). The spectra are consistent with those published in the literature.[62]

2-(2-Fluoroethoxy)-5-iodo-3-methoxybenzoic Acid (3). Compound 1 (0.943 g, 3.66 mmol) was dissolved in dried acetone (40 mL), and potassium carbonate (1.5 g, 10.86 mmol) was added, followed by 1-bromo-2-fluoroethane (2.5 g, 19.68 mmol). The mixture was refluxed with stirring for 48 h. Acetone was evaporated and the residue was dissolved in dichloromethane, washed several times with water, and dried over anhydrous sodium sulfate. Dichloromethane was evaporated under reduced pressure. The crude product was purified by column chromatography (silica gel, ethyl acetate/petroleum ether, 20/80) to obtain 0.9 g (86%) of compound 2. The ester 2 was hydrolyzed to the acid 3 by a method based on the published procedure[30] to provide a white solid in 79% yield: mp 125–126 °C; FT-IR (KBr) ν 3450 (br, OH), 1740 (strong, CO); ^{1}H NMR ($CDCl_3$) δ 8.05 (d, 1 H), 7.39 (d, 1 H), 4.78 (m, 1 H), 4.68 (m, 1 H), 4.52 (m, 1 H), 4.46 (m, 1 H), 3.88 (s, 3 H). Anal. Calcd (CI, high-resolution spectrum) for $C_{10}H_{10}O_4IF$ (M + H) 339.96, found 339.96.

(*S*)-(−)-2-(2-Fluoroethoxy)-5-iodo-3-methoxy-*N*-[(1-ethyl-2-pyrrolidinyl)methyl]benzamide, FIDA1 (4). Acid 3 (0.50 g, 1.47 mmol) was dissolved in dichloromethane (12 mL). The reaction solution was cooled to 0 °C and oxalyl chloride (0.45 mL, 5.1 mmol) was added, followed by DMF (30 μL).[30] The solution was stirred at 0 °C for 30 min and concentrated in a rotary evaporator (bath temperature ~30 °C). The slightly yellow, solid acid chloride was redissolved in dichloromethane (12 mL). To this acid chloride solution was added the amine (*S*)-(−)-*N*-ethyl-2-(aminoethyl)pyrrolidine (0.30 g, 2.9 equiv). After stirring at room temperature for 20 min, the solvent was evaporated under reduced pressure. The residue was redissolved in dichloromethane, washed with 5% $NaHCO_3$, dried over anhydrous sodium sulfate, and filtered; the solvent was removed under reduced pressure. The crude oil product was purified by column chromatography (silica gel, CH_2Cl_2/MeOH, 90/10) to afford 4 (0.52 g, 81%) as an oil: $[\alpha]_D = -43.710°$ (c = 4.25, MeOH); MS m/z 451 (M + H); FT-IR (neat) ν 3400 (br, NH of amide), 1660 (strong, CO); ^{1}H NMR ($CDCl_3$) δ 8.04 (br, 1 H), 8.01 (d, 1 H, J = 1.84 Hz), 7.27 (d, 1 H, J = 1.90 Hz), 4.70 (m, 1 H), 4.60 (m, 1 H), 4.32–4.28 (m, 2 H), 3.86 (s, 3 H), 3.75 (dddd, 1 H), 3.27 (dt, 1 H), 3.18 (m, 1 H), 2.89 (sext, 1 H), 2.70 (m, 1 H), 2.26 (sext, 1 H), 2.18 (q, 1 H), 1.89 (m, 1 H), 1.71 (m, 2 H), 1.62 (m, 1 H), 1.11 (t, 3 H); ^{13}C NMR ($CDCl_3$) δ 163.84, 152.90, 145.62, 131.79, 128.85, 123.95, 87.42, 82.72, 81.36, 77.25, 76.99, 76.74, 72.62, 72.47, 62.74, 59.32, 53.47, 50.61, 48.28, 41.77, 28.35, 22.51, 13.53; optical purity = 100%, t_R = 12.28 min (chiralcel OD, 10% ethanol/hexane, 1 mL/min). Anal. Calcd for $C_{25}H_{36}IO_9N_2F$ (tartrate salt) C, H, N.

5-Iodo-2,3-dimethoxybenzoic Acid (5). The procedure is the same as the synthesis of 2, except that methyl iodide was used as an O-alkylation agent. After workup and purification, the methyl 5-iodo-2,3-dimethoxybenzoate was obtained in 96% yield. The final compound 5 was obtained in 81% yield: mp 118–119 °C (lit.[62] mp 117–118 °C). The spectra are the same as those published in the literature.[62]

(*S*)-(−)-2-(Fluoromethoxy)-3-methoxy-*N*-[(1-ethyl-2-pyrrolidinyl)methyl]-5-(tri-*n*-butylstannyl)benzamide (7). FIDA1 (4, 0.52 g, 1.19 mmol) was dissolved in triethylamine (10 mL). Palladium(0) acetate (0.02 g, 0.089 mmol), and tetrakis-(triphenylphosphine)palladium(0) (0.045 g, 0.039 mmol) were added, followed by bis(tributyltin) (1.04 mL, 2.05 mmol). The mixture was heated to 95–100 °C (oil bath) for 2.5 h. The black reaction mixture was filtered and the black solid washed with triethylamine. The filtrate was evaporated under reduced pressure (temperature < 50 °C). The oil residue was purified by column chromatography (silica gel, EtOAc/MeOH/NH_4OH, 90/10/1) to afford a clear oil of 7 (0.31 g, 42%): FT-IR (neat) ν 3400

(C=O), 3000–2800 (very strong, nonaromatic CH), 1670 (strong, C=O); ^{1}H NMR ($CDCl_3$) δ 8.08 (br, NH), 7.74 (s, 1 H), 7.06 (s, 1 H), 4.76 (m, 1 H), 4.66 (m, 1 H), 4.35–4.26 (m, 2 H), 3.79 (s, 3 H), 3.77 (dddd, 1 H), 3.28 (br, 1 H), 3.18 (br, 1 H), 2.91 (br, 1 H), 2.30 (br, 1 H), 2.19 (br, 1 H), 1.90 (br, 1 H), 1.70 (br, 2 H), 1.13 (t, 3 H), 1.54–0.84 (m, 27 H); ^{13}C NMR ($CDCl_3$) δ 166.28, 151.63, 145.76, 138.08, 130.50, 126.08, 122.96, 82.95, 81.59, 77.23, 76.97, 76.72, 72.47, 72.32, 64.10, 56.06, 53.52, 49.12, 41.50, 30.74, 29.0–9.69 (18 peaks). Anal. Calcd for $C_{29}H_{51}FN_2O_3Sn$ C, H, N.

(*R*)-(+)-2,3-Dimethoxy-*N*-[[1-(4′-fluorobenzyl)-2-pyrrolidinyl]methyl]-5-iodobenzamide, FIDA2 (6). Acid **3** (0.262, 0.84 mmol) was dissolved in dichloromethane (6 mL), and the solution was cooled to 0 °C. To this acid solution were added triethylamine (0.15 mL, 1.10 mmol) and ethyl chloroformate (0.1 mL, 1.0 mmol) in dichloromethane (2 mL) during stirring at 0 °C. After 1 h, a mixture of (*R*)-(+)-2-(aminomethyl)-1-(4-fluorobenzyl)pyrrolidine (0.208 g, 1.0 mmol) and triethylamine (0.15 mL, 1.10 mmol) in dichloromethane (5 mL) was added to the reaction solution. The mixture was stirred at 0 °C for another 1.5 h; the solvent was evaporated under reduced pressure. The residue was redissolved in dichloromethane, washed three times with water, and dried over anhydrous sodium sulfate. The solvent was rotoevaporated, and the crude product was purified by column chromatography (silica gel, CH_2Cl_2/MeOH/NH_4OH, 95/5/1) to obtain 0.348 g (82%) of FIDA2 **6**: $[\alpha]_D$ = +71° (*c* = 3, MeOH); MS *m/z* 516 (M^+) FT-IR (neat) ν 3399 (medium, C=O), 1660 (strong, C=O); ^{1}H NMR ($CDCl_3$) δ 8.35 (br, 1 H), 7.68 (d, 1 H), 7.26 (m, 2 H), 6.96 (m, 3 H), 3.97 (d, 1 H), 3.88 (s, 3 H), 3.84 (s, 3 H), 3.81 (dd, 1 H), 3.31 (d, 1 H), 3.24 (d, 1 H), 2.91 (br, 1 H), 2.75 (br, 1 H), 2.17 (br, 1 H), 1.94 (m, 1 H), 1.68 (br, 2 H), 1.59 (s, 1 H); optical purity = 100%, t_R = 11.92 min (chiralcel OD, 10% ethanol/hexane, 1 mL/min). Anal. Calcd for $C_{25}H_3IO_9N_2F$ (tartrate salt) C, H, N.

(*R*)-(+)-2,3-Dimethoxy-*N*-[[1-(4′-fluorobenzyl)-2-pyrrolidinyl]methyl]-5-(tri-*n*-butylstannyl)benzamide (9). Using the same procedure as for the synthesis of compound **7**, 45% of the desired product was obtained: ^{1}H NMR ($CDCl_3$) 8.30 (br, CO), 7.73 (d, 1 H, *J* = 1.08 Hz), 7.22 (m, 2 H), 7.04 (d, 1 H, *J* = 0.97 Hz), 6.90 (m, 2 H), 2.94 (d, 1 H), 3.82 (s, 3 H), 3.79 (m, 1 H), 3.78 (s, 3 H), 3.20 (dt, 1 H), 3.17 (d, 1 H), 2.85 (br, 1 H), 2.71 (br, 1 H), 2.11 (q, 1 H), 2.09 (m, 1 H), 1.64 (m, 3 H), 1.48–0.80 (m, 27 H). Anal. Calcd for $C_{38}H_{51}O_3N_2FSn$ C, H, N.

(*R*)-(−)-2,3-Dimethoxy-5-iodo-*N*-(2-pyrrolidinylmethyl)-benzamide (15). (R)-(+)-Prolinamide **11**, was converted to (*R*)-(+)-*N*-tritylprolinamine, **12**, using the procedure published in the literature,[55] but with trityl bromide instead of trityl chloride. Compound **12** was reduced to (*R*)-(−)-*N*-tritylprolinamide, **13**, using sodium borohydride, acetic acid, and dioxane.[53] Amine **12** was condensed with acid **5** on the same basis as the synthesis of compound **6**, to afford *N*-tritylbenzamide (**14**). Compound **14** was treated with hydrogen chloride in ethanol to give **15** in 65% yield: $[\alpha]_D$ = −8.4 °C (*c* = 1.4, MeOH); mp 200–202 °C (hydrochloride salt); FT-IR (KBr) ν 3390 (br, NH), 3300 (sharp, NH (amide)), 1660 (strong, C=O); ^{1}H NMR ($CDCl_3$) δ 8.29 (br, NH), 7.95 (d, 1 H, *J* = 1.95 Hz), 7.25 (d, 1 H, *J* = 1.99 Hz), 3.90 (s, 3 H), 3.84 (s, 3 H), 3.57 (m, 1 H), 3.47 (m, 1 H), 3.39 (m, 1 H), 3.00 (m, 2 H), 1.93 (m, 1 H), 1.83 (m, 1 H), 1.78 (m, 1 H), 1.50 (m, 1 H); optical purity = 100%, t_R = 8.75 min (chiralcel OD, 10% ethanol/hexane, 1 mL/min). Anal. Calcd for $C_{14}H_{20}ClIO_3N$ C, H, N.

^{123}I or ^{125}I Labeling. Aqueous hydrogen peroxide (50 μL, 3% w/v) was added to a mixture of 50 μL of compound **7** or **9** (1 mg/mL of EtOH), 50 μL of 0.1 N HCl, and 5 μL of [^{125}I]- or [^{123}I]sodium iodide (2–3 mCi, no carrier added) in a sealed vial. The reaction was allowed to proceed at 23 °C for 30 min, after which it was terminated by the addition of 0.1 mL of sodium bisulfite (300 mg/mL). The reaction mixture was neutralized via the addition of saturated $NaHCO_3$ solution and then extracted with ethyl acetate (3 × 1 mL). The combined organic layers were passed through an anhydrous sodium sulfate column (0.2 cm × 5 cm) and evaporated to dryness by a stream of nitrogen. The residue was dissolved in 100% ethanol (50–100 μL), and the desired product, [^{125}I]- or [^{123}I]FIDA (**8** or **10**), was isolated from unreacted **7** or **9** and a small amount of unknown radioactive impurities by HPLC, using a reverse-phase column (PRP-1, Hamilton, Inc.) and an isocratic solvent 90% acetonitrile/10% pH 7.0 buffer (5 mM, 3,3-dimethylglutaric acid). The appropriate fractions were collected, condensed, and extracted with ethyl acetate (1 × 3 mL). The solution containing the no-carrier-added product was evaporated to dryness and the residue was dissolved in 100% ethanol (purity > 97%, 75% overall yield). The no-carrier-added products, after dilution with saline, were used for the in vivo and in vitro studies.

^{18}F Labeling. [^{18}F]-**19** was prepared by N-alkylation of **15** with [^{18}F]-4-fluorobenzyl iodide using a modification of the published method.[58] No-carrier-added aqueous [^{18}F]fluoride (115 mCi) was prepared by the University of Pennsylvania JSW BC 3015 cyclotron via the ^{18}O(p,n)^{18}F nuclear reaction on a small volume enriched-water (98%) target. The target material was passed through an AG1-X8 (Bio-Rad) anion exchange resin (hydroxide form, 20–30 mg) and converted into [^{18}F]-CsF by elution with 0.5 mL of aqueous cesium carbonate (4 mg/mL) into a glass reaction vessel. The water was removed in vacuo at 90 °C under a stream of nitrogen and the [^{18}F]CsF was redissolved in a solution of 200 μL of DMSO/7 μL water. A mixture of **16** in 100 mL of DMSO was added and the reaction mixture was heated at 120 °C for 10 min.[59] Following Sep pak purification, the [^{18}F]-4-fluorobenzaldehyde, **17**, was converted to 4-[^{18}F]-fluorobenzyl iodide, **18**, according to the published method.[59] N-Alkylation of **15** was performed by heating a mixture of **15** and **18** in 500 mL of DMF at 90 °C for 10 min. The crude product was purified by C18 reversed-phase HPLC (0.1 M ammonium formate/methanol, 20:80) to give 6.8 mCi of [^{18}F]-**19** (10% radiochemical yield decay corrected to SOS). The total synthesis time was 130 min and the specific activity of [^{18}F]**19** was ~800 mCi/μmol. The radiochemical purity was >99%.

Biodistribution in Rats. Male Sprague–Dawley rats (225–300 g), allowed free access to food and water, were used for in vivo biodistribution study. While the rats were under ether anesthesia, 0.2 mL of a saline solution containing [^{123}I]FIDA **8** or **10** (8–10 μCi) was injected directly into the femoral vein, and rats were sacrificed at various time points postinjection by cardiac excision under ether anesthesia. The organs of interest were removed and weighed and the radioactivity was counted with a Packard γ automatic counter (Model 5000). The percentage dose per organ was calculated by a comparison of the tissue counts to suitably diluted aliquots of the injected material. Total activities of blood and muscle were calculated under the assumption that they were 7% and 40% of the total body weight, respectively.

Regional brain distribution in rats was obtained after an iv injection of [^{123}I]FIDA **8** or **10**. By dissecting, weighing, and counting samples from different brain regions (cortex, striatum, hippocampus, and cerebellum), the percentage dose/gram of the sample was calculated by comparing the sample counts with the court of the diluted initial dose. The uptake ratio of each ratio was obtained by dividing the percentage dose/gram of each region by that of the cerebellum.

In Vitro Binding. Rat tissue homogenates were prepared as described previously.[26,27] The binding assays were performed by incubating 50 μL of tissue preparations containing 40–60 μg of protein with appropriate amounts of ^{125}I-labeled ligand and competitors in a total volume of 0.2 mL of the assay buffer. After an incubation period of 15 min at 37 °C (with stirring), the samples were rapidly filtered in a cell harvester (Brandel M-24R) under vacuum through Whatman GF/B glass-fiber filters pretreated with 0.2% protamine base and washed with 3 × 5 mL of cold (4 °C) 50 mM Tris-HCl buffer, pH 7.4. The nonspecific binding was obtained in the presence of 10 μM (+)-butaclamol. The filters were counted in a γ-counter at an efficiency of 70%. Both Scatchard and competition experiments were analyzed with the iterative nonlinear least squares curve-fitting program LIGAND.[63]

In Vivo SPECT and PET Imaging of Monkey Brain. Male cynomologus monkeys (~5 lbs) were anesthetized with ketamine (10–20 mg/kg) and maintained on a 1% Isoflurane/99% oxygen mixture throughout the imaging procedure. No carrier-added [^{18}F]- or [^{123}I]FIDA2 in saline was administered in the saphenous vein. Series of SPECT or PET images were obtained on a Picker prism camera (using fan beam collimation, 20% window, set at 159 keV, a similar imaging parameter as that reported previously for SPECT).[57] Tomographic slices 4 mm thick were obtained, and counts in different regions, i.e. basal ganglia, cortex, and cerebellum, were obtained. For PET imaging studies, a PENN-

PET is used and data for different brain regions were obtained using a similar regions of interest analysis.[64]

Acknowledgment. This work is supported by grants awarded by NIH (NS-24538, MH-48539). Authors thank Catherine Cartwright and Karen Loomis for their editorial assistance.

References

(1) Seeman, P. Brain dopamine receptors. *Pharmacol. Rev.* **1980**, *32*, 229–269.

(2) Seeman, P.; Niznik, H. B. Dopamine receptors and transporters in Parkinson's disease and schizophrenia. *FASEB J.* **1990**, *4*, 2737–2744.

(3) Mazière, B.; Coenen, H. H.; Haldin, C.; Nagren, K.; Pike, V. W. PET radioligands for dopamine receptors and re-uptake sites: Chemistry and biochemistry. *Nucl. Med. Biol.* **1992**, *19*, 497–512.

(4) Fowler, J. S.; Wolf, A. P. New directions in positron emission tomography. *Ann. Rep. Med. Chem.* **1989**, *24*, 277–283.

(5) Fowler, J. S.; Wolf, A. P.; Volkow, N. D. New directions in positron emission tomography-part-II. *Ann. Rep. Med. Chem.* **1990**, *25*,l 261–268.

(6) Sedvall, G. PET Imaging of Dopamine Receptors in Human Basal Ganglia: Relevance to Mental Illness. *Trends Neurol. Sci.* **1990**, *13*, 302–308.

(7) Wong, D. F.; Kuhar, M. J. In vivo PET and SPECT receptor imaging: New technology and tactics for receptor measurement. *Adv. Exp. Med. Biol.* **1988**, *236*, 181–193.

(8) Kung, H. F. Overview of radiopharmaceuticals for diagnosis of central nervous disorders. *Crit. Rev. Clin. Lab. Sci.* **1991**, *28*, 269–286.

(9) Farde, L.; Wiesel, F.-A.; Hall, H.; Halldin, C.; Stone-Elander, S.; Sedvall, G. No D_2 Receptor Increase in PET Study of Schizophrenia. *Arch. Gen. Psychiatry* **1987**, *44*, 671–672.

(10) Farde, L.; Weisel, F.-A.; Stone-Elander, S.; Halldin, C.; Nordström, A.-L.; Hall, H.; Sedvall, G. D_2 Dopamine Receptors in Neuroleptic-Naive Schizophrenic Patients. A PET Study with [^{11}C]raclopride. *Arch. Gen. Psychiatry* **1990**, *47*, 213–219.

(11) Wong, D.; Wagner, H., Jr.; Tune, L.; Dannals, R.; Pearlson, G.; Links, J.; Tamminga, C.; Broussole, E.; Ravert, H.; Wilson, A.; Toung, J.; Malat, J.; Williams, J.; O'Tuama, L.; Snyder, S.; Kuhar, M.; Gjedde, A. Positron Emission Tomography Reveals Elevated D_2 Dopamine Receptors in Drug-Naive Schizophrenics. *Science* **1986**, *234*, 1558–1563.

(12) Wagner, H. N.; Burns, H. D.; Dannals, R. J. Imaging dopamine receptors in the human brain by positron tomography. *Science* **1983**, *221*, 1264–1266.

(13) Wong, D.; Wagner, H., Jr.; Pearlson, G.; Dannals, R.; Links, J.; Ravert, H.; Wilson, A.; Suneja, S.; Bjorvvinsen, E.; Kuhar, M.; Tune, L. Dopamine Receptor Binding of C-11-3-N-Methylspiperone in the Caudate in Schizophrenia and Bipolar Disorder: A Preliminary Report. *Psychopharmacol. Bull.* **1985**, *21*, 595–598.

(14) Young, L. T.; Wong, D. F.; Goldman, S.; Minkin, E.; Chen, C.; Matsumura, K.; Scheffel, U.; Wagner, H. N., Jr. Effects of endogenous dopamine on kinetics of 3H N-methylspiperone and 3H raclopride binding in the rat brain. *Synapse* **1991**, *9*, 188–194.

(15) Dewey, S. L.; Logan, J.; Wolf, A. P.; Brodie, J. D.; Angrist, B.; Fowler, J. S.; Volkow, N. D. Amphetamine induced decreases in [^{18}F]-N-methylspiperone binding in the baboon brain using positron emission tomography (PET). *Synapse* **1991**, *7*, 321–327.

(16) Andreasen, N.; Carson, R.; Diksic, M.; Evans, A.; Farde, L.; Gjedde, A.; Hakim, A.; Lal, S.; Nair, N.; Sedvall, G.; Tune, L.; Wong, D. Workshop on Schizophenia, PET, and Dopamine D_2 Receptors in the Human Neostriatum. *Schizophr. Bull.* **1988**, *14*, 471–484.

(17) Wong, D. F.; Tune, L.; Shaya, E.; Pearlson, G.; Yung, B.; Dannals, R. F.; Wilson, A. A.; Ravert, H. T.; Wagner, H. N. J.; Gjedde, A. The comparison of dopamine receptor density measured by C-11 raclopride and NMSP in the same living human brain (abstract). *J. Nucl. Med.* **1992**, *33*, 847.

(18) Budinger, T. F. Advances in emission tomography: Quo Vadis? *J. Nucl. Med.* **1990**, *31*, 628–631.

(19) De Paulis, T.; Hall, H.; Ögren, S.-O.; Wägner, A.; Stensland, B.; Csöregh, I. Synthesis, Crystal Structure and Antidopaminergic Properties of Eticlopride (FLB 131). *Eur. J. Med. Chem.—Chim. Ther.* **1985**, *29*, 273–276.

(20) Högberg, T.; Ramsby, S.; Ögren, S.-O; Norinder, U. New Selective Dopamine D-2 Antagonists as Antipsychotic Agents. *Acta Pharm. Suec.* **1987**, *24*, 289–328.

(21) Högberg, T.; Ström, P.; De Paulis, T.; Stensland, B.; Csöregh, I.; Lundin, K.; Hall, H.; Ögren, S. Potential antipsychotic agents. 9. Synthesis and stereoselective dopamine D-2 receptor blockade of a potent class of substituted (R)-N-[(1-Benzyl-2-pyrrolidinyl)-methyl]benzamides. Relations to other side chain congeners. *J. Med. Chem.* **1991**, *34*, 948–955.

(22) Högberg, T.; Bengtsson, S.; De Paulis, T.; Johansson, L.; Ström, P.; Hall, H.; Ögren, S. Potential antipsychotic agents. 5. Synthesis and antidopaminergic properties of substituted 5,6-dimethoxysalicylamides and related compounds. *J. Med. Chem.* **1990**, *33*, 1155–1163.

(23) Farde, L.; Eriksson, L.; Blomquist, S.; Halldin, C. Kinetic Analysis of Central [^{11}C]Raclopride Binding to D_2-Dopamine Receptors Studied by PET—A Comparison to the Equilibrium Analysis. *J. Cereb. Blood Flow Metab.* **1989**, *9*, 696–708.

(24) Hall, H.; Kohler, C.; Gawell, L.; Farde, L.; Sedvall, G. Raclopride a new selective ligand for the dopamine D_2 receptors. *Prog. Neuro-Psychopharm. Biol. Psychiatry* **1988**, *12*, 559.

(25) Kung, H. F.; Kasliwal, R.; Pan, S.; Kung, M. P.; Mach, R. H.; Guo, Y. Z. Dopamine D-2 receptor imaging radiopharmaceuticals: Synthesis, radiolabeling and in vitro binding of R-(+) and S-(−)-3-iodo-2-hydroxy-6-methoxy-N-[(1-ethyl)-2-pyrrolidinyl)methyl]-benzamide (IBZM). *J. Med. Chem.* **1988**, *31*, 1039–1043.

(26) Kung, M.-P.; Kung, H. F.; Billings, J.; Yang, Y.; Murphy, R.; Alavi, A. The Characterization of IBF as a New Selective Dopamine D-2 Receptor Imaging Agent. *J. Nucl. Med.* **1990**, *31*, 648–654.

(27) Murphy, R.; Kung, H.; Kung, M.-P.; Billings, J. Synthesis and Characterization of Iodobenzamide Analogues: Potential D-2 Dopamine Receptor Imaging Agents. *J. Med. Chem.* **1990**, *33*, 171–178.

(28) Kessler, R.; Ansari, M.; De Paulis, T.; Schmidt, D.; Clanton, J.; Smith, H.; Manning, R.; Gillespie, D.; Ebert, M. High Affinity Dopamine D_2 Receptor Radioligands. 1. Regional Rat Brain Distribution of Iodinated Benzamides. *J. Nucl. Med.* **1991**, *32*, 1593–1600.

(29) Kessler, R.; Ansari, M.; Schmidt, D.; De Paulis, T.; Clanton, J.; Innis, R.; Al-Tikriti, M.; Manning, R.; Gillespie, D. High Affinity Dopamine D2 Receptor Radioligands. 2. [^{125}I]Epidepride, a Potent and Specific Radioligand for the Characterization of Striatal and Extrastriatal Dopamine D_2 Receptors. *Life Sci.* **1991**, *49*, 617–628.

(30) Bishop, J.; Mathis, C.; Gerdes, J.; Whitney, J.; Eaton, A.; Mailman, R. Synthesis and in vitro evaluation of 2,3-dimethoxy-5-(fluoroalkyl)-substituted benzamides: High affinity ligands for CNS dopamine D-2 receptors. *J. Med. Chem.* **1991**, *34*, 1612–1624.

(31) Mathis, C.; Bishop, J.; Gerdes, J.; Faggin, B.; Mailman, R. Synthesis of Aryl-Substituted 5-[^{18}F]Fluoroalkylbenzamides: High Affinity Ligands for Dopamine D-2 Studies. *J. Lab. Compd. Radiopharm.* **1991**, *30*, 357–359.

(32) Mukherjee, J.; Perry, B.; Cooper, M. Fluorinated Benzamide Neuroleptics. 1. Radiosynthesis of (S)-N-[(1-Ethyl-2-Pyrrolidinyl)Methyl]-5-(2[F-18]Fluoroethyl)-2-Methoxybenzamide: A Potential Fluorine-18 Labeled PET Radiotracer for Dopamine D2 Receptors. *J. Lab. Compd. Radiopharm.* **1990**, *28*, 609–616.

(33) Mukherjee, J.; Luh, K.; Yasillo, N.; Perry, B.; Levy, D.; Chen, C.-T.; Ortega, C.; Beck, R.; Cooper, M. Dopamine D-2 Receptors Imaged by PET in Cebus Apella Using [^{18}F]Benzamide Neuroleptic. *Eur. J. Pharmacol.* **1990**, *175*, 363–364.

(34) Högberg, T.; Ström, P.; Hall, H.; Köhler, C.; Halldin, C.; Farde, L. Syntheses of [^{123}I]-, [^{125}I]- and Unlabelled (S)-3-Iodo-5,6-Dimethoxy-N-[(1-Ethyl-2-Pyrrolidinyl)Methyl]Salicylamide (NCQ 298), Selective Ligands for the Study of Dopamine D-2 Receptors. *Acta Pharm. Nord.* **1990**, *2*, 53–60.

(35) Hall, H.; Högberg, T.; Halldin, C.; Köhler, C.; Ström, P.; Ross, S.; Larsson, S.; Farde, L. NCQ 298, A New Selective Iodinated Salicylamide Ligand for the Labelling of Dopamine D_2 Receptors. *Psychopharmacology* **1991**, *103*, 6–18.

(36) Saji, H.; Nakatsuka, I.; Shiba, K.; Tokui, T.; Horiuchi, K.; Yoshitake, A.; Torizuka, K.; Yokoyama, A. Radioiodinated 2'-Iodospiperone: A New Radioligand for In Vivo Dopamine Receptor Study. *Life Sci.* **1987**, *41*, 1999–2006.

(37) Yonekura, Y.; Iwasaki, Y.; Saji, H.; Iida, Y.; Magata, Y.; Konishi, J.; Fujita, T.; Sadato, N.; Tsuchida, T.; Tamaki, N.; Fukuyama, H.; Shibasaki, H.; Yokoyama, A. SPECT Imaging of D-2 dopamine receptors in human brain with 2'-Iodospiperone: Initial clinical studies (abstract). *J. Nucl. Med.* **1992**, *33*, 897.

(38) Mazière, B.; Loc'h, C.; Raynaud, C.; Hantraye, P.; Stulzaft, O.; Syrota, A.; Mazière, M. I-123 Iodolisuride, a New SPECT Imaging Ligand for Brain Dopamine D_2 Receptors. *J. Nucl. Med.* **1989**, *30*, 731–732.

(39) Chabriat, H.; Samson, Y.; Vidailhet, M.; Levasseur, M.; Loc'h, C.; Mazière, B.; Zilbovicius, M.; Bonnet, A. M.; Agid, Y.; Bourguignon, M.; Raynaud, C.; Syrota, A. SPECT Imaging of dopamine D2 receptors with [^{123}I]iodolisuride (ILIS) in supranuclear palsy (abstract). *J. Nucl. Med.* **1992**, *33*, 1019.

(40) Verhoeff, N. P.; Brucke, T.; Podreka, I.; Bobeldijk, M.; Angelberger, P.; Van Royen, E. A. Dynamic SPECT in two healthy volunteers to determine the optimal time for in vivo D_2 dopamine receptor imaging with ^{123}I-IBZM using the rotating gamma camera. *Nucl. Med. Commun.* **1991**, *12*, 687–697.

(41) Tatsch, K.; Schwartz, J.; Oertel, W.; Kirsch, C.-M. SPECT imaging of dopamine D2 receptors with I-123 IBZM in parkinsonian syndromes. *J. Nucl. Med.* **1991**, *32*, 1014–1015.

(42) Konig, P.; Benzer, M.; Fritzsche, H. SPECT technique for visualization of cerebral dopamine D2 receptors. *Am. J. Psychiatry* **1991**, *148*, 1607–1608.

(43) Costa, D. C.; Verhoeff, N. P.; Cullum, I. D.; Ell, P. J.; Syed, G. M.; Barrett, J.; Palazidou, E.; Toone, B.; Van Royen, E.; Bobeldijk, M. In vivo characterization of 3-iodo-6-methoxybenzamide ^{123}I in humans. *Eur. J. Nucl. Med.* **1990**, *16*, 813–816.

(44) Cordes, M.; Henkes, H.; Laudahn, D.; Brāu, H.; Kramp, W.; Girke, W.; Hierholzer, J.; Eichstädt, H.; Felix, R. Initial experience with SPECT examinations using [^{123}I]IBZM as a D_2-dopamine receptor antagonist in Parkinson's disease. *Eur. J. Radiology* **1991**, *12*, 182–186.

(45) Brücke, T.; Podreka, I.; Angelberger, P.; Wenger, S.; Topitz, A.; Küfferle, B.; Müller, C.; Deecke, L. Dopamine D_2 Receptor Imaging with SPECT: Studies in different neuropsychiatric disorders. *J. Cereb. Blood Flow Metab.* **1991**, *11*, 220–228.

(46) Billings, J.; Broich, K.; Shao, L.; Mozley, D.; Guo, Y. Z.; Kung, H. F. Preclinical Study of I-123 IBF: A SPECT Agent for CNS D_2 Dopamine Receptor (abstract). *J. Nucl. Med.* **1992**, *5*, 870.

(47) Verhoeff, N.; Speelman, J.; van Royen, E.; de Jong, J. In vivo dopamine D2-receptors imaging with I-123 iodobenzamide SPECT in patients with multiple system atrophy. *Eur. Nucl. Med. Meet.* **1991**, 520.

(48) Wilson, A.; Dannals, R.; Ravert, H.; Wagner, H., Jr. Preparation of [^{11}C]- and [^{125}I]IMB: a dopamine D-2 receptor antagonist. *Appl. Radiat. Isot.* **1989**, *40* (5), 369–73.

(49) Sánchez-Roa, P.; Grigoriadis, D.; Wilson, A.; Sharkey, J.; Dannals, R.; Villemangne, V.; Wong, D.; Wagner, Jr., H.; Kuhar, M. [^{125}I]Spectramide: A Novel Benzamide Displaying Potent and Selective Effects at the D_2 Dopamine Receptor. *Life Sci.* **1989**, *45*, 1821–1829.

(50) Banks, W. R.; Moerlein, D.; Parkinson, D.; Welch, M. J. 6-O-[F-18]Flouroalkylated analogues of raclopride: potential radiopharmaceuticals for mapping cerebral D-2 receptors with PET (abstract). *J. Nucl. Med.* **1991**, *32*, 1096.

(51) Halldin, C.; Högberg, S.; Bengtsson, H.; Hall, H.; Farde, L. Synthesis of [^{18}F] NCQ 115, a new selective reversible D-2 dopamine receptor ligand for PET (abstract). *J. Lab. Compd. Pharm.* **1991**, *30*, 355–356.

(52) Edgar, K. J.; Falling, S. N. An Efficient and Selective Method for the Preparation of Iodophenols. *J. Med. Chem.* **1990**, *18*, 5287–5291.

(53) Högberg, T.; Ramsby, S.; Ström, P. Efficient stereoconservative synthesis of 1-substituted (S)- and (R)-2-aminomethylpyrrolidines. *Acta Chem. Scand.* **1989**, *43*, 660–664.

(54) Chumpradit, S.; Kung, H. F.; Billings, J.; Kung, M. P.; Pan, S. (±)-7-Chloro-8-hydroxy-1-(4′-[125I]iodophenyl)-3-methyl-2,3,4,5-tetrahydro-1H-3-benzazepine (TISCH): A high affinity and selective iodinated ligand for CNS D-1 dopamine receptor. *J. Med. Chem.* **1991**, *34*, 877–883.

(55) Florvall, L.; Ögren, S.-O. Potential Neuroleptic Agents. 2,6-Dialkoxybenzamide Derivatives with Potent Dopamine Receptor Blocking Activities. *J. Med. Chem.* **1982**, *25*, 1280–1286.

(56) Hanson, R.; Tonneson, G.; McLaughlin, W. Electrophilic radioiododestannylation as a new radioiodination method. **1981**, *18*, 128–129.

(57) Billings, J.; Kung, M. P.; Chumpradit, S.; Mozley, D.; Alavi, A.; Kung, H. F. Characterization of radioiodinated TISCH: A high affinity and selective ligand for mapping CNS dopamine D-1 receptor. *J. Neurochem.* **1991**, *58*, 227–236.

(58) Haka, M.; Kilbourn, M.; Watkins, G.; Toorongian, S. Aryltrimethylammonium trifluoromethanesulfonates as precursors to aryl [18F]fluorides: Improved synthesis of [^{18}F]GBR-13119. *J. Lab. Compd. Radiopharm.* **1988**, *27*, 823–833.

(59) Mach, R.; Scripko, J.; Ehrenkaufer, R.; Morton, T. The use of [F-18]4-fluorobenzyl iodide as a prosthetic group for introducing F-18 into pharmacologically active molecules: N-Alkylation of amines and amides. *J. Lab. Compd. Radiopharm.* **1991**, *30*, 154–155.

(60) Kung, H.; Guo, Y. Z.; Billings, J.; Xu, X.; Mach, R.; Blau, M.; Ackerhalt, R. Preparation and Biodistribution of [^{125}I]IBZM: A Potential CNS D-2 Dopamine Receptor Imaging Agent. *Nucl. Med. Biol.* **1988**, *15*, 195–201.

(61) Kung, H.; Pan, S.; Kung, M.-P.; Billings, J.; Kasliwal, R.; Reilley, J.; Alavi, A. In vitro and in vivo evaluation of [^{123}I]IBZM: A potential CNS D-2 dopamine receptor imaging agent. *J. Nucl. Med.* **1989**, *30*, 88–92.

(62) Yue, E.; Gerdes, J.; Mathis, C. Synthesis of 2,3-dimethoxy-5-iodobenzoic acid. *J. Org. Chem.* **1991**, *56*, 5451–5456.

(63) Munson, P.; Rodbard, D. LIGAND: A Versatile Computerized Approach for Characterization of Ligand-Binding Systems. *Anal. Biochem.* **1980**, *107*, 220–239.

(64) Karp, J. S.; Muellenhner, G.; Mankoff, D. L. Continuous-slice-PENN-PET. *J. Nucl. Med.* **1990**, *31*, 617–627.